RSC Advances

This article can be cited before page numbers have been issued, to do this please use: H. Guo, Y. Li, J. Zheng, J. Gan, L. Liang, K. Wu and M. Lu, *RSC Adv.*, 2015, DOI: 10.1039/C5RA10957D.

ROYAL SOCIETY OF CHEMISTRY

www.rsc.org/advances

View Article Online
DOI: 10.1039/C5RA10957D

High thermo-responsive shape memory epoxies based on substituted biphenyl mesogenic with good water resistance

Huilong Guo,[a,b] Yinwen Li,[a,b] Jian Zheng,[a,b] Jianqun Gan,[a,b] Liyan Liang,[a] Kun Wu,[a] Mangeng Lu,[a] *

[a] Key Laboratory of Cellulose and Lignocellulosics Chemistry, Chinese Academy of Sciences; Guangzhou Institute of Chemistry, Chinese Academy of Sciences, Guangzhou 510650, PR China

[b] University of Chinese Academy of Sciences, Beijing 100049, PR China

Correspondence to: Mangeng Lu (E-mail: *mglu@gic.ac.cn*)

ABSTRACT

In this work, a novel epoxy monomer denoted as 3,5'-Di-t-butyl-5,3'-dimethyl biphenyl diglycidyl ether (t-BuMBPDGE) was synthesized and applied into situ composites with 3,3',5,5'-tetramethyl-4,4'-biphenyl Diglycidyl ether (TMBPDGE), accompanied with curing agent aromatic amines. The liquid crystalline phase structure and the crosslink density of substituted biphenyl epoxies were determined by polarized optical microscopy, wide angle X-ray diffraction measurements and dynamic storage moduli data. The samples showed good mechanical properties and could recover quickly from a second state to their initial states with shape fixity ratio higher than 98% and shape recovery ratio higher than 99%, owing to the oriented structure and increased crosslink network density caused by the orientation of biphenyl mesogenic. The high glass transition temperatures ranging from 160 to 178℃ and good water resistance could make contribute to a stable fixed shape. The water resistance is analyzed by contact angles test. The samples exhibited contact angles of 92-98 degrees, which indicated that the water resistance was apparently better than that of conventional epoxy systems.

KEYWORDS: shape memory; liquid crystalline epoxy; substituted biphenyl mesogenic

1.INTRODUCTION

Shape memory polymers (SMPs)[1-13] are stimuli-sensitive polymers that are capable of changing their shapes from a temporary state to their original or permanent shape after being exposed to the external stimulus such as heat, light, pH, solvents, electric field or magnetic field. Among various stimuli responsive SMPs, thermo-responsive SMPs are the most attractive due to their numerous applications in biomedical field[14-18], information carriers[19, 20], assembly/disassembly[21, 22], actuators[23-25], and aerospace[26, 27].

Low transition temperature (below 100°C) and elastomeric polymers, thermoplastic polyurethanes (TPU) for example, have been primarily investigated in the research of thermo-responsive SMPs, which are suitable for the applications in biomedical field. Martin Bothe et al[28] used 4,4′-methylenediphenyl diisocyanate, 1,4-butanediol as a chain extender to develop three physically cross-linked, phase-segregated poly(ester urethane) with differing hard to soft segment ratios,

View Article Online
DOI: 10.1039/C5RA10957D

gaining control over programmable thermo-responsiveness. Higher moisture resistance and switching temperatures of SMPs are often required in the application in aerospace or structural components. Ying Shi et al[29] developed high thermo-responsive thermoplastic SMPs based on metal salts of sulfonated PEEK (M-SPEEK) ionomers with transition temperatures as high as 250 °C, but not every M-SPEEK exhibited high shape fixity and recovery efficiencies during each cycle. Thermoset polymer systems are the most studied materials as high thermo-responsive SMPs exhibiting high shape fixity and recovery efficiencies.[30-32]

Shape memory epoxies, as the chemically cross-linked shape memory polymers, have so many desirable characteristics, such as good thermal and mechanical properties, ease of processability, composite forming properties and very good dimensional stability, which make shape memory epoxy polymers attractive for application in the processing of many smart engineering systems.[33, 34] Gao et al[31] prepared a high thermo-responsive (at 150 °C) thermoset epoxy polymer modified with poly(ether ether ketone). Fan, Wang Kun et al [35] prepared a type of thermal-induced shape memory polymer using a new epoxy resin-polybutadiene epoxy (PBEP) and bisphenol A-type cyanate ester (BACE) in different mass ratios with Tg ranging from 136 to 165℃, owing to varying cross-linking density affected by a flexible long-carbon chain structure of PBEP. Tao Xie et al[36] represented a facile method to precisely tune the Tg of epoxy SMPs decreasing from 89℃ to room temperature by either reducing the crosslink density or introducing flexible aliphatic epoxy chains. Agustina B. Leonardi et al[4] reported an epoxy network with chemical and physical cross-links which showed an excellent behavior as an SMP enabling a combination of relatively high tensile strains and recovery stresses. Hendrik Lützen et al[37] studied novel segmented and covalently cross-linked epoxy/poly(ε-caprolactone) (PCL) polymers which showed a shape memory effect; the covalently cross linked epoxy network acts as hard segment to store the permanent shape for the recovery process, and the reversible process of crystallization and melting in the PCL segment acts as switch for deformation and fixation in the segment. However, conventional cross-linked epoxy polymers (or epoxy based SMPs) were highly water absorbing (about 1–4 wt%) and hydrophilic (water contact angle of 50–52 degrees) owing to the existence of large number of hydroxyl groups in the cross-linked networks. Kumar, K. S. [8] reported hydrophobic shape memory poly(oxazolidone-triazine) cyclomatrix networks with water contact angles of 82-86 degrees and transition temperatures between 127 and 180℃.

Liquid crystalline epoxides (LCEs), owning oriented and chemically cross-linked networks which are formed from curing of low molecular weight, rigid rod epoxy monomers with curing agents of aromatic amine, are superior to conventional amorphous epoxies in the performance of better mechanical properties, better dimensional stability, lower coefficients of thermal expansion, increased fracture toughness and noticeable high temperature properties.[38-44] It was reported that the oriented structure of LCEs could increase packing density of the segments, resulting in increased crosslink network density.[45, 46] And the increasing crosslinking density could significantly improve the shape memory properties.[47] In addition, the free volume of polymer could be decreased through the

View Article Online
DOI: 10.1039/C5RA10957D

closely packed arrangement of mesogens, leading to dramatically reduced solvent absorptions.[41, 48] Therefore, it was attractive that biphenyl mesogenics were induced into cross linked epoxy systems, to gain high-Tg and good water resistance shape memory epoxy resins. However, there were only few works that were focused on the shape memory effect of hydrophobic liquid crystalline epoxies.[49, 50]

In this paper, novel epoxy monomers containing biphenyl mesogenics were synthesized and a series of high-Tg and good water resistance shape memory epoxy resins based on substituted biphenyl mesogenic were prepared and characterized. Moreover the relationship between structure and water resistance and shape memory properties was investigated in our work.

2. EXPERIMENTAL

2.1 Materials

4,4'-Diaminodiphenylmethane (DDM, See Scheme 1) was purchased from Aladdin and was used as curing agent. 2,6-xylenol and 2-tert-butyl-6-methyl-phenol were supplied by Aladdin. Tetrabutyl ammonium bromide, periodic acid and sodium hydrosulfite were purchased from laboratory Text & Industrial Measurement Instruments multi-source. All other reagents were of analytical grade and used as received.

2.2 Epoxy monomer synthesis

2.2.1 Synthesis of 3,3',5,5'-tetramethyl-4,4'-biphenyl Diglycidyl ether [TMBPDGE, abbreviated as (1)]

Diglycidyl ether of 3,3',5,5'-tetramethyl-4,4'-biphenyl (See Scheme 1) was synthesized in our laboratory according to our early reports.[51] The chemical structure of the product was evaluated by means of ^{1}H NMR and FTIR (KBr pellet, cm^{-1}) techniques. IR: 912 (epoxy C-O, st), 1380 (aromatic CH_3, band), 1579 and 1477 (aromatic C=C, st). ^{1}H-NMR ($CDCl_3$, in ppm): 7.15–7.17 (d, 4H, aromatic), 2.32–2.34 (d, 12H, CH_3), 4.03–4.06, 3.74–3.78 (dd, 4H, CH_2, glycidyl), 3.34–3.38 (m, 2H, CH, epoxy), 2.87-2.87, 2.70–2.72 (tdd, 4H, CH_2, epoxy). The epoxy equivalent of the product was determined by the HCl/acetone titration to be 198 (theoretical, 177). The melting point of (1) measured by DSC was 102℃.

2.2.2 Synthesis of 3,5'-Di-t-butyl-5,3'-dimethyl biphenyl diglycidyl ether [t-BuMBPDGE, abbreviated as (2)]

(2) was synthesized through refluxing 8 g of (0.0245 mol) 3,5'-Di-t-butyl-5,3'- dimethyl biphenyldiol with excess epichlorohydrin (32.5 g, 0.275 mol) and 20 ml of isopropanol catalyzed by tetrabutyl ammonium bromide (0.24 g, 0.744 mmol) under nitrogen atmosphere at 85 ℃ till the solution was clear. Then a 12 g of 30 wt NaOH aqueous solution was added dropwise into the mixture. The excess epichlorohydrin, water and isopropanol were evaporated under reduced pressure after 1 h. Finally, the product was extracted by dichloromethane and washed with water and water/methanol

View Article Online
DOI: 10.1039/C5RA10957D

(9/1 volume) mixture three times respectively, then dried over $MgSO_4$. A product at a 91% yield was obtained after filtration and removal of dichloromethane. The chemical structure of the product was evaluated by means of ^1H NMR and FTIR (KBr pellet, cm^{-1}) techniques. IR: 912 (epoxy C-O, st), 1380 (aromatic CH_3, band), 1579 and 1477 (aromatic C=C, st).^1H-NMR (CDCl3, in ppm) : 7.15–7.25 (d, 4H, aromatic) ,2.32–2.34 (s, 6H, CH_3) ,4.03–4.06, 3.74–3.78 (dd, 4H, CH_2, glycidyl) ,3.34–3.38 (m, 2H, CH, epoxy) , 2.87–2.87, 2.70–2.72 (tdd, 4H, CH_2, epoxy) , 1.34-1.41 (d, 18H, CH_3). The epoxy equivalent of the product was determined by the HCl/acetone titration to be 263 (theoretical, 219). The softening point of (2) evaluated by DSC was 10.5℃.

3,5'-Di-t-butyl-5,3'-dimethyl biphenyldiol was prepared using oxidative coupling reaction in which 2-tert-butyl-6-methyl-phenol was oxidated by periodic acid. 2-tert-butyl-6-methyl- phenol (5 g, 30.44 mmol), dissolved by 5 ml of dimethylformamide, was added into a 100 mL round-bottom flask with a magnetic stirring bar at a temperature of 80℃, then 10.96 g of 40 wt% periodic acid aqueous solution was added dropwise into the mixture. Stop heating till lots of bubbles occurred, one hour later the mixture was precipitated by 500 ml of water. And the precipitation was identified as 3,5'-Di-t-butyl-5,3'-dimethyl diphenoquinone after being filtrated, washed with water and dried. Then 4 g (0.012 mol) of 3,5'-Di-t-butyl-5,3'-dimethyl diphenoquinone and excess sodium hydrosulfite (3 g), dissolved in 20 ml of 80 wt% ethanol aqueous solution, was stirring for 1 h at 80℃ till the solution turned yellowish clear. Finally precipitation identified as 3,5'-Di-t-butyl-5,3'-dimethyl biphenyldiol was obtained after adding the solution into 500ml of water, filtration, washing the precipitation with water and being dried under vacuum.

2.3 Curing of substituted biphenyl epoxies

The stoichiometric amount of epoxy monomer (different weight ratios of (1) and (2)) and DDM were dissolved in dichloromethane, then dichloromethane was removed under reduced pressure at room temperature, the samples were cured at low temperature of 105 ℃ which is the isotropic temperature of (1)/DDM mixtures, for 5 h to ensure the totally reaction of linear chain extension and post-cured at 160℃ for 4 h, 200℃ for 1 h to guarantee completely branching and crosslinking. After curing, the cured products were extracted from the mold, to be tested. An absorption peak at 912 cm^{-1} was observed characteristic of the epoxy stretching in the FTIR spectrum of (1) and (2), while this absorption peak at 912 cm^{-1} could not be found in the spectrums of (1)/DDM, (2)/DDM and (1)/(2)/DDM composites (See Figure 2). These indicated all the samples were completely cured.

2.4 Physical measurements

The ^1H NMR was obtained with a DRX-400 spectrometer with $CDCl_3$ as a solvent and tetramethylsilane (TMS) as an internal standard.

Calorimetric measurements were performed using a Perkin–Elmer Diamond DSC calorimeter, under nitrogen atmosphere to measure the heat flow under nonisothermal conditions. Samples of about 10 mg were sealed in aluminium pans. A first thermal cycle heating from 40 to 250℃ and a cooling

View Article Online
DOI: 10.1039/C5RA10957D

scan from (250 to 40 °C) was performed to eliminate thermal history. After that, a new heating scan from 40 to 250℃ was performed to determine the glass transition temperature (Tg) and the melting point. All the scans were performed at a heating/cooling rate of 20 ℃/min.

The liquid crystalline phase structure of substituted biphenyl epoxies was examined by a polarized light optical microscopy (POM) (Orthoglan, LEITZ, Germany) and wide angle X-ray diffraction measurements (WAXS) which were carried out with a Rigaku Diffractometer (D/MAX-1200), using monochromatic Cu Karadiation (40 kV, 30 mA) and secondary graphite monochromator, with the X-ray scatting intensities being detected by a scintillation counter incorporating a pulse-height analyzer.

The tensile test at room temperature (30℃) was carried out by an Instron mechanical testing machine (SHT5000, Shenzhen SANS Testing Machine) at a strain rate of 2 mm/min. The Young's modulus, break strength, and elongation at break were obtained from the stress–strain curves. The sample dimensions were 100 mm * 10 mm *0.6 mm.

Infrared spectra, recorded on a WQF-410 Fourier Transform Infrared (FTIR) spectrometer in the wavenumber range from 4000 to 400 cm^{-1} at 25℃ were used to investigate the change of epoxy ring before and after curing. The spectra were collected after 32 scans. The time interval between each spectrum collected was 60 s.

The response of the samples to small-strain mechanical deformation was measured as a function of temperature (-120 to 200℃) using a NETZSCH DMA 242 dynamic mechanical analyzer in a tensile mode. The testing was carried out at a heating rate of 5℃/min in a N_2 atmosphere, frequencies of 1 Hz, a dynamic stress of 5 N, and a static stress of 0.5 N. The sample displacement was 30 μm. Storage moduli (E'), loss moduli (E"), and loss tangent (tan δ) were recorded.

The shape memory properties was tested as following: the sample was cut into 80mm*10mm*0.6mm Strips; then the strips were put into silicone oil at a temperature 20 ℃ higher than the Tg of the sample for 30 minutes; later the strips were bended around a tube (Peripheral curvature**,** 7.24/dm^{-1}), quenched to room temperature with a constant external force; finally the shape recovery process of bended strips were observed in silicone oil at a temperature 20 ℃ higher than the Tg of the sample. The shape recovery process were recorded by a camera (SONY, DSC-RX100 M2)**,** then the video was divided into 25 pictures per second using Corel VideoStudio Pro X4 software. The shape recovery curvature of the strips was determined by bidimensional measurement software, through which the shape fixity ratio and shape recovery ratio were calculated using the following equations. The shape memory cycles were determined by repeating the above process (shape fixity, shape recovery) 5 times for each sample. Repeated to test three samples for each test condition and selected averages.

$$R_f = (R-R_0) / (R_t-R_0) \quad (1)$$

$$R_r = (R-R') / (R-R_0) \quad (2)$$

View Article Online
DOI: 10.1039/C5RA10957D

R_f: shape fixity ratio

R_r: shape recovery ratio

R: curvature of the sample after fixed

R_t: curvature of the tube(7.24/dm^{-1})

R_0: curvature of the initial state of the sample

R': Curvature of the recovered sample

3. RESULTS AND DISCUSSION

3.1. The liquid crystalline phase structure of substituted biphenyl epoxies

The polarized optical microscopic pictures after curing of (1)/DDM and (2)/DDM were shown in Figure 3. Birefringence was observed from both of the POM pictures of (1)/DDM and (2)/DDM network. And bright droplet-like domains of the liquid crystalline were dispersed in (2)/DDM network while (1)/DDM illustrated a "schlieren-like" texture with a higher disclination density.

To further investigate the nematic structure of biphenyl epoxies affected by substituents, wide angle X-ray diffraction patterns of (1)/DDM, (2)/DDM and (1)/(2)/- DDM composites were analyzed, as shown in Figure 4. It could be seen that all the samples showed broad peaks around 23° with broader peak in (2)/DDM than that in (1)/DDM.

C.B. McARDLE[52] reported that the X-ray diffraction patterns of nematic polymers showed generally a typical broad peak in the region of 2θ= 15-30°, owing to the average lateral distance between the neighboring chains with d-spacing of 3-5 Å. All of the (1)/DDM, (2)/DDM and (1)/(2)/DDM composites illustrated a typical nematic characteristic with broad peaks around 23° corresponding to d-spacing of 3.9 Å. Curing of liquid crystalline epoxies included linear chain extension at early stage, then branching, and finally crosslinking, which could have significant effects on orientation of mesogenic and structure of liquid crystalline epoxy resins. During linear chain extension stage, the mobility and orientation of mesogen units were hindered by steric hindrance of the methyl substituents or tert-butyl substituents, so that the smectic LC phase could not be formed in all the samples. While in the first stage of curing at 105℃ which was much lower than the DSC exothermic temperature of the reaction of epoxy and DDM, the mesogen units could be oriented with great efforts in their isotropic state before branching and crosslinking. Although during mesogen units orientation stage, steric hindrance of the tert-butyl substituents was larger than that of methyl substituents, the reactivity of (2) and DDM might be lower than that of (1) and DDM. Thus, the (2)/DDM resin could stay in isotropic state longer than (1)/DDM resin, which was observed during curing process that (1)/DDM resin changed from isotropic state to solid membrane earlier than (2)/DDM resin. Moreover, the softening point of (2) was much lower than (1), during heating process, the orientation of (2) started earlier than that of (1), all of these led to a similar nematic LC phase in all the samples with more slightly oriented structure in (1)/DDM resin.

Uniaxial oriented nematic structure mode of (1)/DDM network was shown schematically in Figure 5. From which the orientation of substituted biphenyl mesogenic could be more easily analyzed and understood.

View Article Online
DOI: 10.1039/C5RA10957D

3.2. The crosslink density of substituted biphenyl epoxies

For ideal networks, Gaussian network model method can be used to determine the level of crosslinking.

$$E_R'=3\rho RT/Mc$$

Where Mc is total sample weight that contains one mole of elastically effective network chains, E_R' is the storage modulus at Tg+50℃, T is the absolute temperature of Tg+50K, **ρ is the** density of the samples, and R is the gas constant.

The crosslink density can be defined as the number of moles of elastically effective network chains per cubic centimeter of sample which was denoted as v_e

$$Mc = \rho/v_e$$

So that the Gaussian network model can be changed into the following equation [53]

$$v_e=E'/3RT$$

The calculated crosslink density v_e was shown in Table 1, from which it could be seen that the crosslink density decreased as the increasing of the content of (2). This could be easily explained that network segments packing was hampered by larger substituents of tert-butyl in (2)/DDM resin than methyl substituents in (1)/DDM resin, resulting in the highest v_e in (1)/DDM resin.

3.3. The mechanical properties of substituted biphenyl epoxies

Figure 6 showed the relationships between the tensile stresses versus strain at room temperature. It was observed from Figure 6 that the modulus increased with the decreasing of the content of (1), while the tensile strength and the elongation at break decreased with the increasing of the content of (2), as was illustrated in Table 2. And it was shown in Figure 7 that the dynamic storage moduli (E') of (2)/DDM at room temperature reached the highest position, over 1000MPa higher than the lowest one of (1)/DDM resin.

The mechanical properties in the glass state mainly depended on the van der Waals interactions.[54] Ortiz et al. indicated that glass deformation at small strains involved bending and small angular rotations of network strands. [55] With stress increasing, the biphenyl mesogenic could be aligned along the direction of force, resulting in an enhancement in the packing density of polymer chains, so that the intermolecular resistance to rotation, shear might be enhanced. Therefore, the mechanical properties could be improved by the alignment of biphenyl mesogenic along the direction of force. It could be concluded that All of the (1)/DDM, (2)/DDM and (1)/(2)/DDM composites illustrated a similar nematic characteristic with d-spacing of 3.9 Å. Thus, the orientation of biphenyl mesogenic along the direction of stress was more difficult in the (2)/DDM resin than in (1)/DDM resin, owing to larger steric hindrance of the tert-butyl substituents in (2)/DDM resin with similar d-spacing of about 3.9 Å for all the samples, which could be confirmed though comparing the XRD data before and after tensile test,

View Article Online
DOI: 10.1039/C5RA10957D

as were illustrated in Figure 4 and Table 3. After tensile test, the nematic d-spacing changed from 3.9 Å to 2.67 Å in (1)/DDM resin, while in (2)/DDM resin the nematic d-spacing only cut back 0.13 Å, which indicated that biphenyl mesogenic was more easily oriented along the direction of stress in (1)/DDM resin. Thus, the tensile strength of (1)/DDM resin was reinforced owing to the orientation of biphenyl mesogenic in the direction of stress. And the modulus could be enhanced in the oriented direction with stress increasing, so that the slope of the tensile stresses versus strain curve of (1)/DDM resin increased with increasing of stress. However, the slope of the tensile stresses versus strain curve of (1)/DDM resin at first stage was lower than that of (2)/DDM resin, which was because the orientation of biphenyl mesogenic along the direction of stress was obstructed by the larger steric hindrance of the tert-butyl substituents in (2)/DDM resin, resulting in higher modulus, higher dynamic storage moduli (E') and lower elongation at break of (2)/DDM than that of (1)/DDM resin.

3.4. The glass transition temperature (Tg) of substituted biphenyl epoxies

The glass transition temperature of the samples was determined by DSC, as was shown in Figure 8. It could be seen that the glass transition temperature of the samples decreased from 178℃ to 158℃ with the content of (2) increasing. The Tg of the samples were also confirmed by DMA and the results were shown in Figure 7 and Table 1.

As was well known, Tg referred to the temperature at which the network segments began to move. And the movement of network segments could be influenced by the chemical crosslinking, physical entanglement and the packing density of the segments. In our work orientation of substituted biphenyl mesogenics could increase packing density of the segments, resulting in increased crosslink network density. The interchain interactions can be enhanced owing to the increased packing density of the segments, making the substituted biphenyl mesogens slip and rotate not easily. Therefore, higher glass transition temperatures than that of conventional epoxy systems (the Tg of bisphenol-A/DDM system was 155℃, reported by Bin Li [56]) were obtained, which acted an important role in the stable fixed shape. As discussed above, more slightly oriented structure existed in (1)/DDM resin and the crosslink density decreased as the increasing of the content of (2), moreover, larger substituents of tert-butyl in (2)/DDM resin could weaken the interchain interactions and made the mesogens slip and rotate easily. Thus, glass transition temperature of the samples increased with the content of (2) decreasing.

3.5. The water resistance properties of substituted biphenyl epoxies

The water resistance properties of substituted biphenyl epoxies were determined by contact angle test, as was shown in Figure 9. It could be seen that the contact angle of the samples increased from 92 degree to 98 degree with the content of (1) increasing.

Kumar, K. S. [8] reported hydrophobic shape memory poly(oxazolidone-triazine) cyclomatrix networks with water contact angles of 82-86 degrees, which are higher than that for typical epoxy systems. As was discussed above, the orientation of substituted biphenyl mesogenics could contribute to an

View Article Online
DOI: 10.1039/C5RA10957D

increased crosslink network density, resulting in closely packed polymer chains. Thus, the water resistance property was enhanced with the content of (1) increasing owing to more oriented and closely packed network in (1)/DDM system.

3.6. The shape memory properties of substituted biphenyl epoxies

The shape recovery process and the shape recovery curvature of the strips were shown in Figure 10 and Figure 11. While the shape fixity ratio, shape recovery ratio and shape recovery time of (1)/DDM, (2)/DDM and (1)/(2)/DDM composites during different shape memory cycles were illustrated in Table 4. It could be found that the shape recovery process of (1)/DDM resin was the fastest and that became slower with the increase of the content of (2). All the samples could be almost completely fixed and recovered with shape recovery ratio higher than 98% and shape recovery ratio higher than 99% in the first shape memory cycle. And it could be seen that all the samples still showed an ideal shape memory properties with shape fixity ratio higher than 97% and shape recovery ratio higher than 98%. Which indicated all the samples showed a very good reproducibility and stability of the shape memory behavior. Figure 12 showed the shape recovery process of (2)/DDM from 30℃ to 176℃ in silicone oil at a heating rate of 10℃/min. It could be observed that the shape recovery process hardly happened below 160℃. And the sample gradually recovered to its original state from 160℃ to 176℃. Moreover, as shown in Table 5, the samples showed an extremely low uptake of silicone oil. Therefore, it was the temperature change that triggered the shape changes of the samples rather than oil uptake.

There was oriented and chemically cross-linked structure in substituted biphenyl epoxies. The oriented mesogen and chemically crosslink network made substituted biphenyl epoxy resins an excellent shape memory material, with higher shape fixity ratio (98%) and shape recovery ratio (99%) and extremely fast shape recovery process within 37 s. This shape memory effect is driven by the entropic behavior in the substituted biphenyl segments between the crosslinks of the epoxy. Below Tg, the substituted biphenyl segments between the network points could not change any conformation and were locked into the orientational order network permanently unless a suitably large mechanical force was applied (comparing the XRD data before and after tensile test, as were illustrated in Figure 4 and Table 3). The rotational conformations of substituted biphenyl segments could be changed at relatively lower stresses when heated above Tg. Above Tg, the substituted biphenyl segments could aligned in the direction of stresses, increasing the stored energy in the epoxy as the entropy of the epoxy chains decreased. Upon cooling in the deformed shape, the epoxy chains could no longer freely rotate. The substituted biphenyl segments then recovered this stored energy by returning to the initial high entropy configuration when the samples were heated above Tg.[57-59] Larger substituents of tert-butyl in (2)/DDM resin might play a negative role in the alignment of substituted biphenyl segments in the direction of stresses above Tg, so upon cooling in the deformed shape, the stored energy and the entropy configuration change of (2)/DDM resin would not be as obvious as that of (1)/DDM resin. Moreover, during shape recovery process, the shape recovery

View Article Online
DOI: 10.1039/C5RA10957D

stresses might be directly proportional to the innerstress. According to the ideal elasticity equation, the stress increased with the elasticity modulus under the condition of a same strain, the storage moduli at temperature 20℃ higher than Tg of (1)/DDM resin was higher that of (2)/DDM resin, so that the innerstress is of (1)/DDM resin is higher that of (2)/DDM resin at same strains. Thus, the shape recovery stress of (1)/DDM resin was expected to be higher than that of (2)/DDM resin, eventually, the shape recovery process was accelerated with the increase of content of (1).

4. CONCLUSION

~~Quick~~ Thermo-responsive shape memory epoxy resins based on substituted biphenyl mesogenic were prepared and characterized in this work. The good mechanical and water resistance properties and extraordinary shape memory properties with high shape memory transition temperatures, shape fixity ratio higher than 98% and shape recovery ratio higher than 99%, indicating a new idea to prepare hydrophobic shape memory materials by introducing the mesogenic units into epoxy resins in the application of **self-deployable antennae**.

More slightly oriented structure could be formed in the (1)/DDM resin, and the crosslink density decreased as the content of (2) increasing, which was attribute to larger steric hindrance of the tert-butyl substituents in (2).

The modulus and the dynamic storage moduli increased with the decreasing of the content of (1), while the tensile strength and the elongation at break decreased with the increasing of the content of (2). The biphenyl mesogenic was more easily oriented along the direction of stress in (1)/DDM resin, while the orientation of biphenyl mesogenic was obstructed by the larger steric hindrance of the tert-butyl substituents in (2)/DDM resin, resulting in higher modulus, higher dynamic storage moduli (E') and lower elongation at break of (2)/DDM than that of (1)/DDM resin. Moreover, the tensile strength of (1)/DDM resin was reinforced owing to the orientation of biphenyl mesogenic in the direction of stress.

The glass transition temperatures, water resistance properties and the shape recovery speed of the samples were enhanced with the increase of the content of (1), owing to more oriented structure and increased crosslink network density caused by the orientation of biphenyl mesogenic in (1)/DDM resin.

ACKNOWLEDGEMENTS

This research was supported by the intergration of Industry Education and Research of Guangdong Province project (2011A091000007) and the National Natural Science Foundation of China (20974121)

REFERENCES

1. **H. Meng and G. Q. Li, *Polymer*, 2013, 54, 2199-2221.**
2. **H. M. Chen, Y. Liu, T. Gong, L. Wang, K. Q. Zhao and S. B. Zhou, *Rsc Adv*, 2013, 3, 7048-7056.**

View Article Online
DOI: 10.1039/C5RA10957D

3. Q. H. Meng and J. L. Hu, *Compos Part a-Appl S*, 2009, 40, 1661-1672.
4. A. B. Leonardi, L. A. Fasce, I. A. Zucchi, C. E. Hoppe, E. R. Soule, C. J. Perez and R. J. J. Williams, *Euro Polym J*, 2011, 47, 362-369.
5. Y. Li, H. Guo, Y. Zhang, J. Zheng, J. Gan, X. Guan and M. Lu, *Rsc Adv*, 2014, 4, 17768-17779.
6. J. Hu, Y. Zhu, H. Huang and J. Lu, *Prog Polym Sci*, 2012, 37, 1720-1763.
7. J. Leng, X. Lan, Y. Liu and S. Du, *Prog Mater Sci*, 2011, 56, 1077-1135.
8. K. S. S. Kumar and C. P. R. Nair, *Rsc Adv*, 2014, 4, 2969-2973.
9. T. Xie, *Polymer*, 2011, 52, 4985-5000.
10. C. Liu, H. Qin and P. T. Mather, *J Mater Chem*, 2007, 17, 1543-1558.
11. T. Pretsch, *Polymers*, 2010, 2, 120-158.
12. L. Sun, W. M. Huang, Z. Ding, Y. Zhao, C. C. Wang, H. Purnawali and C. Tang, *Mater Design*, 2012, 33, 577-640.
13. G. J. Berg, M. K. McBride, C. Wang and C. N. Bowman, *Polymer*, 2014, 55, 5849-5872.
14. L. Peponi, I. Navarro-Baena, A. Sonseca, E. Gimenez, A. Marcos-Fernandez and J. M. Kenny, *Euro Polym J*, 2013, 49, 893-903.
15. I. Navarro-Baena, J. M. Kenny and L. Peponi, *Cellulose*, 2014, 21, 4231-4246.
16. J.-M. Raquez, S. Vanderstappen, F. Meyer, P. Verge, M. Alexandre, J.-M. Thomassin, C. Jerome and P. Dubois, *Chemistry-a European Journal*, 2011, 17, 10135-10143.
17. A. Saralegi, M. Luz Gonzalez, A. Valea, A. Eceiza and M. Angeles Corcuera, *Compos Sci Technol*, 2014, 92, 27-33.
18. L. Sun and W. M. Huang, *Mater Design*, 2010, 31, 2684-2689.
19. M. Ecker and T. Pretsch, *Rsc Adv*, 2014, 4, 46680-46688.
20. N. Fritzsche and T. Pretsch, *Macromolecules*, 2014, 47, 5952-5959.
21. L. Sun, W. M. Huang, H. B. Lu, C. C. Wang and J. L. Zhang, *Assembly Automation*, 2014, 34, 78-93.
22. D. A. van den Ende, H. J. van de Wiel, W. A. Groen and S. van der Zwaag, *Smart Mater Struct*, 2012, 21, DOI: 10.1088/0964-1726/21/1/015011.
23. M. Bothe and T. Pretsch, *J Mater Chem A*, 2013, 1, 14491-14497.
24. A. Khaldi, J. A. Elliott and S. K. Smoukov, *Journal of Materials Chemistry C*, 2014, 2, 8029-8034.
25. L. Sun, W. M. Huang, C. C. Wang, Z. Ding, Y. Zhao, C. Tang and X. Y. Gao, *Liq Cryst*, 2014, 41, 277-289.
26. Y. Li, J. Li, W. Li and H. Du, *Smart Mater Struct*, 2014, 23, DOI: 10.1088/0964-1726/23/12/123001
27. A. Y. N. Sofla, S. A. Meguid, K. T. Tan and W. K. Yeo, *Mater Design*, 2010, 31, 1284-1292.
28. M. Bothe, F. Emmerling and T. Pretsch, *Macromol Chem Physic*, 2013, 214, 2683-2693.
29. Y. Shi, M. Yoonessi and R. A. Weiss, *Macromolecules*, 2013, 46, 4160-4167.
30. T. H. Tong, *Maleimide based high temperature shape memory polymers. US Pat. Appl. US7276195B1, July 26, 2006.*.
31. J. P. Gao, C. Q. Zhang, X. C. He, H. Y. Ma, X. F. An, X. S. Yi, G. D. Dang and C. H. Chen, *Adv. Mater. Res. 2010, 152-153, 530-535.*
32. P. Mather and C. Liu, *Castable shape memory polymers. US Pat. Appl. US2004/0030062A1, April 29, 2003*.
33. K. S. S. Kumar, R. Biju and C. P. R. Nair, *React Funct Polym*, 2013, 73, 421-430.
34. X. L. Wu, S. F. Kang, X. J. Xu, F. Xiao and X. L. Ge, *J Appl Polym Sci*, 2014, 131.
35. K. Wang, G. Zhu, L. Niu, Y. Wang and Z. Liu, *J Polym Res*, 2014, 21, DOI: 10.1007/s10965-014-0385-8.
36. T. Xie and I. A. Rousseau, *Polymer*, 2009, 50, 1852-1856.
37. H. Luetzen, T. M. Gesing, B. K. Kim and A. Hartwig, *Polymer*, 2012, 53, 6089-6095.
38. M. Wlodarska, A. Maj, B. Mossety-Leszczak, G. W. Bak, H. Galina, L. Okrasa and M. Izdebski, *J Polym Res*, 2013, 20, DOI: 10.1007/s10965-013-0227-0.

View Article Online
DOI: 10.1039/C5RA10957D

39. Y. Li, P. Badrinarayanan and M. R. Kessler, *Polymer*, 2013, 54, 3017-3025.
40. A. Mija and C. N. Cascaval, *Polimery-W*, 2009, 54, 786-789.
41. C. Farren, M. Akatsuka, Y. Takezawa and Y. Itoh, *Polymer*, 2001, 42, 1507-1514.
42. Y. Li and M. R. Kessler, *Polymer*, 2014, 55, 2021-2027.
43. C. Carfagna, E. Amendola and M. Giamberini, *Compos Struct*, 1994, 27, 37-43.
44. G. G. Barclay and C. K. Ober, *Prog Polym Sci*, 1993, 18, 899-945.
45. H. Guo, M. Lu, L. Liang, J. Zheng, Y. Zhang, Y. Li, Z. Li and C. Yang, *J Appl Polym Sci*, 2014, 131, DOI: 10.1002/app.40363.
46. J. Y. Lee and J. Jang, *Polym Bull*, 2007, 59, 261-267.
47. K. Wei, G. Zhu, Y. Tang, T. Liu and J. Xie, *Journal of Materials Research*, 2013, 28, 2903-2910.
48. J. Feng, K. Berger and E. Douglas, *J Mater Sci*, 2004, 39, 3413-3423.
49. T. Shen, F. Wu and C. Sun, *J Macromol Sci A*, 2013, 50, 1085-1090.
50. L. Liang, D. Zhou and M. Lu, in *Advances in Liquid Crystals*, ed. Y. M. Huang, 2010, vol. 428-429, pp. 391-393.
51. S. Ren, L. Liang, Y. Lan and M. Lu, *J Appl Polym Sci*, 2007, 106, 2917-2924.
52. C. McARDLE, *Side Chain Liquid Crystal Polymers; Chapman and Hall: New York, NY, 1989; Chapter 6.*
53. L. W. Hill, *Prog Org Coat*, 1997, 31, 235-243.
54. E. F. Oleinik, *Advances in Polymer Science*, 1986, 80, 49-99.
55. C. Ortiz, R. Kim, E. Rodighiero, C. K. Ober and E. J. Kramer, *Macromolecules*, 1998, 31, 4074-4088.
56. G.-R. Xu, M.-J. Xu and B. Li, *Polym Degrad Stab*, 2014, 109, 240-248.
57. H. Guo, Y. Li, J. Zheng, J. Gan, L. Liang, K. Wu and M. Lu, *J Appl Polym Sci*, 2015, DOI: 10.1002/app.42616.
58. Y. Dong, J. Ding, J. Wang, X. Fu, H. Hu, S. Li, H. Yang, C. Xu, M. Du and Y. Fu, *Compos Sci Technol*, 2013, 76, 8-13.
59. M. Di Prima, K. Gall, D. L. McDowell, R. Guldberg, A. Lin, T. Sanderson, D. Campbel and S. C. Arzberger, *Mech Mater*, 2010, 42, 304-314.

Figure captions

View Article Online
DOI: 10.1039/C5RA10957D

View Article Online
DOI: 10.1039/C5RA10957D

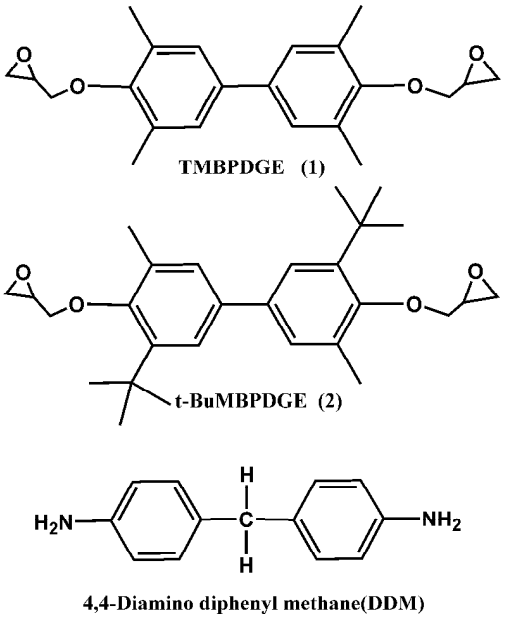

Scheme 1 Chemical structures of (1), (2) and DDM

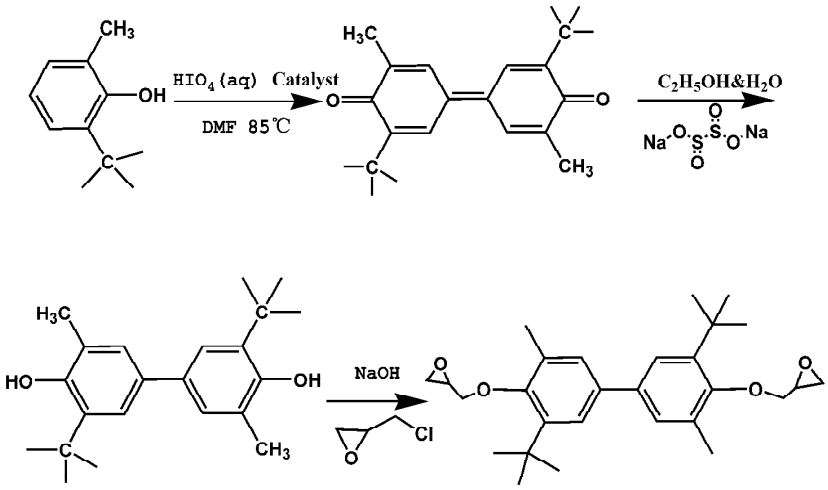

Scheme 2 synthesis of (2)

View Article Online
DOI: 10.1039/C5RA10957D

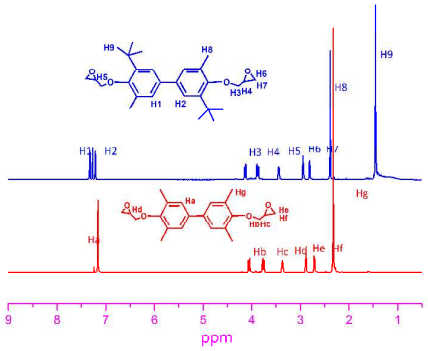

Fig 1 ^{1}H NMR of (1) and (2)

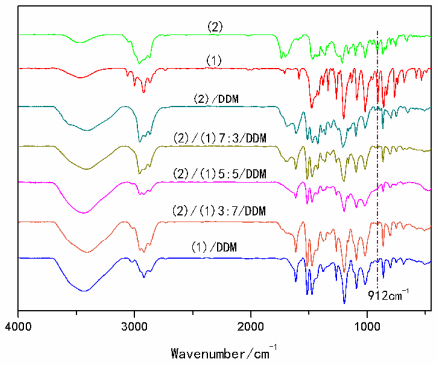

Fig 2 FTIR spectrum of uncured pure (1) and (2), (2)/DDM resin, (1)/DDM resin and (1)/(2)/DDM composites

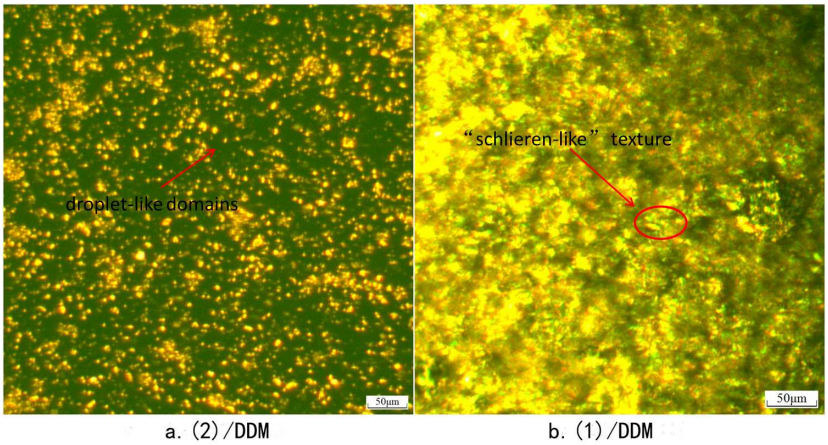

Fig 3 Polarized optical microscopic pictures of (2)/DDM resin and (1)/DDM resin after curing at room temperature

View Article Online
DOI: 10.1039/C5RA10957D

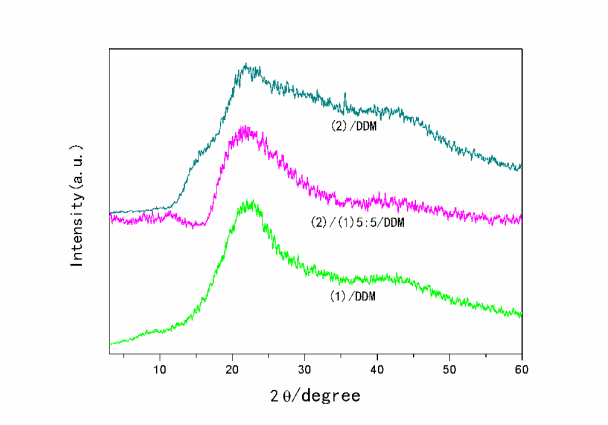

Fig 4 Wide angle X-ray diffraction measurements of (2)/DDM resin, (1)/DDM resin and (1)/(2)/DDM composites

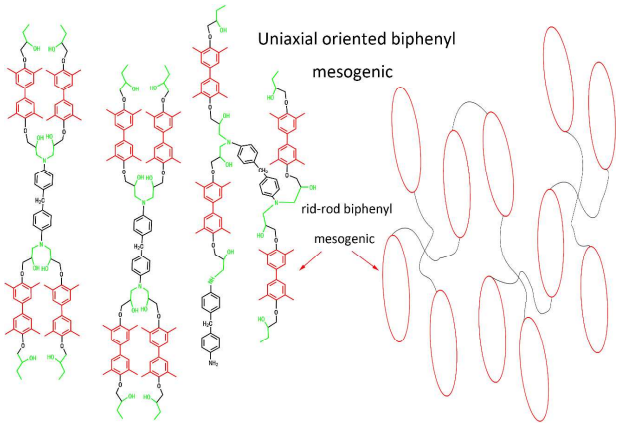

Fig 5 Uniaxial oriented nematic structure mode of (1)/DDM resin

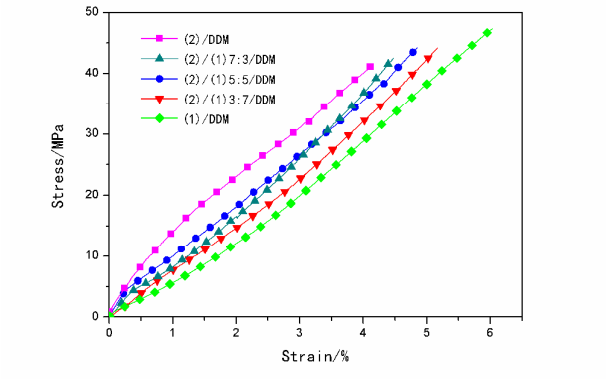

Fig 6 Stress versus strain curves for (2)/DDM resin, (1)/DDM resin and (1)/(2)/DDM composites at room temperature

View Article Online
DOI: 10.1039/C5RA10957D

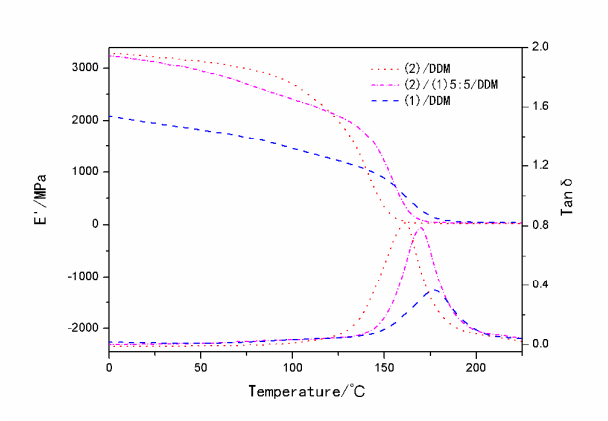

Fig 7 Dynamic storage moduli (E') and loss tangent (tan δ) of (2)/DDM resin, (1)/DDM resin and (1)/(2)/DDM composite

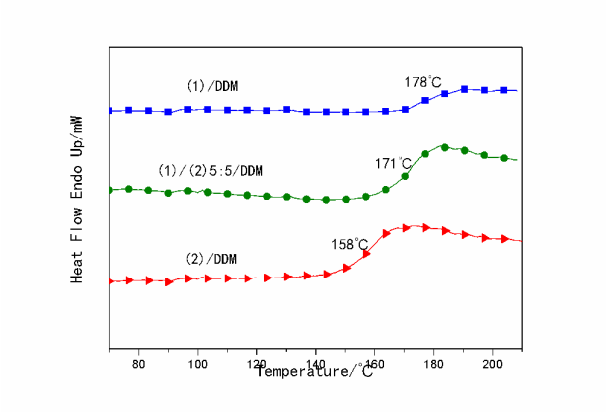

Fig 8 DSC curves for (2)/DDM resin, (1)/DDM resin and (1)/(2)/DDM composite

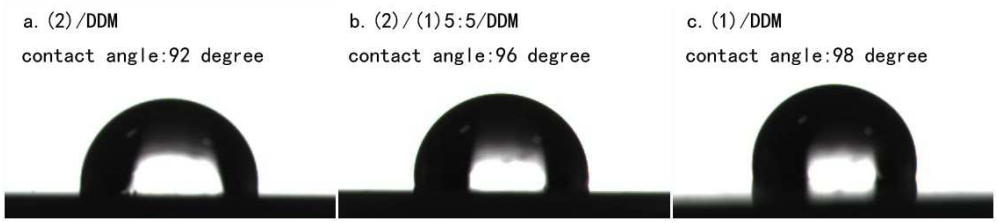

Fig 9 Contact angles of (2)/DDM resin, (1)/DDM resin and (1)/(2)/DDM composite

View Article Online
DOI: 10.1039/C5RA10957D

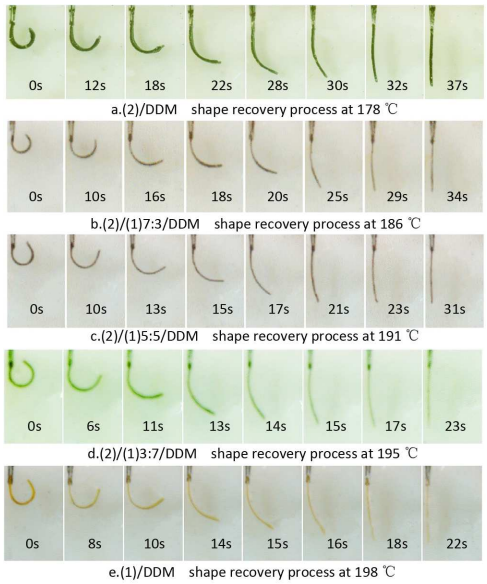

Fig 10 shape recovery process pictures for (2)/DDM resin, (1)/DDM resin and (1)/(2)/DDM composites

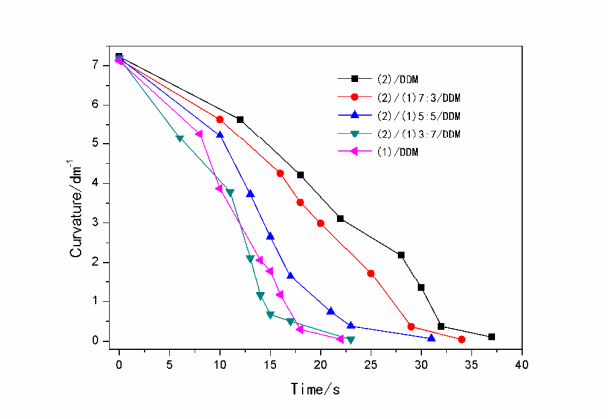

Fig 11 shape recovery curvature versus time for (2)/DDM resin, (1)/DDM resin and (1)/(2)/DDM composites

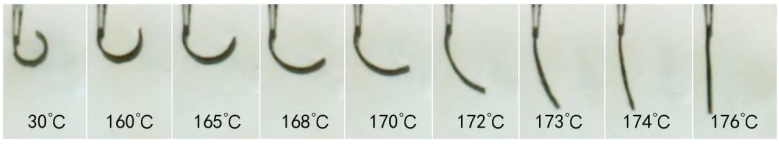

Fig 12 shape recovery process pictures for (2)/DDM from 30℃ to 176℃ in silicone oil at a heating rate of 10℃/min.

View Article Online
DOI: 10.1039/C5RA10957D

Table 1 DMA results and crosslink density of (2)/DDM resin, (1)/DDM resin and (1)/(2) /DDM composite

Samples	Storage moduli (E')(MPa)20℃	(E_R')(MPa) (T_g+50℃)	T_g(℃)	v_e (mol/cm^3)
(1)/DDM	2007	38.03	178	$3.07*10^{-3}$
(2)/(1)5:5/DDM	3145	29.87	169	$2.42*10^{-3}$
(2)/DDM	3215	21.15	160	$1.75*10^{-3}$

View Article Online
DOI: 10.1039/C5RA10957D

Table 2 Tensile results of (2)/DDM resin, (1)/DDM resin and (1)/(2) /DDM composites at room temperature

sample	E(MPa)	ε_b (%)	δ_b (MPa)
(1)/DDM	651	6.03	47.31
(2)/(1)3:7/DDM	712	5.17	44.16
(2)/(1)5:5/DDM	1458	4.85	44.19
(2)/(1)7:3/DDM	1120	4.47	42.48
(2)/DDM	1831	4.12	41.09

View Article Online
DOI: 10.1039/C5RA10957D

Table 3 Data of XRD before and after tensile test of (2)/DDM resin, (1)/DDM resin and (1)/(2) /DDM composites

sample	2θ/°		d/Å	
	beforer tensile test	After tensile test	before tensile test	after tensile test
(1)/DDM	22.5	7.6/33.5	3.95	11.62/2.67
(2)/(1)3:7/DDM	22.0	7.4/29.4	4.05	11.97/3.03
(2)/(1)5:5/DDM	21.8	9.4/23.7	4.08	9.36/3.75
(2)/(1)7:3/DDM	21.6	9.4/23.6	4.12	9.40/3.77
(2)/DDM	21.8	8.52/22.6	4.08	10.38/3.92

View Article Online
DOI: 10.1039/C5RA10957D

Table 4 Shape fixity ratio, shape recovery ratio and shape recovery time of (1)/DDM, (2)/DDM and (1)/(2)/DDM composites during 5 shape memory cycles

N	(1)/DDM			(2)/(1)3:7/DDM			(2)/(1)5:5/DDM			(2)/(1)7:3/DDM			(2)/DDM		
	R_f/%	R_r%	T_r/s	R_f/%	R_r%	T_r/s	R_f/%	R_r%	T_r/s	R_f/%	R_r%	T_r/s	R_f/%	R_r%	T_r/s
1	98.3	99.2	22	98.4	99.3	23	98.4	99.1	31	98.5	99.4	34	98.6	99.1	37
2	98.4	99.1	21	98.3	99.2	25	98.2	99.3	32	98.3	99.2	35	98.5	99.3	38
3	98.2	99.2	24	98.1	99.2	25	98.1	98.9	30	98.2	99.3	36	98.3	99.3	38
4	97.8	98.9	24	97.6	99.0	26	97.3	98.6	34	97.8	98.9	35	97.7	98.6	39
5	97.6	98.5	26	97.5	98.4	25	97.2	98.3	35	97.4	98.3	39	97.6	98.2	41

View Article Online
DOI: 10.1039/C5RA10957D

Table 5 silicone oil uptake of (2)/DDM resin, (1)/DDM resin and (1)/(2) /DDM composites at 200℃

Samples	silicone oil uptake for 10min /(%)	silicone oil uptake for 30min /(%)	silicone oil uptake for 60min /(%)
(1)/DDM	0.21	0.43	0.62
(2)/(1)5:5/DDM	0.24	0.47	0.66
(2)/DDM	0.27	0.51	0.71